Journal of Power Sources 270 (2014) 608–618

Contents lists available at ScienceDirect

Journal of Power Sources

journal homepage: www.elsevier.com/locate/jpowsour

# Various supercritical carbon dioxide cycle layouts study for molten carbonate fuel cell application

Seong Jun Bae, Yoonhan Ahn, Jekyoung Lee, Jeong Ik Lee*

*Department of Nuclear and Quantum Engineering, Korea Advanced Institute of Science and Technology, 373-1 Guseong-dong, Yuseong-gu, Daejeon 305-701, Republic of Korea*

## HIGHLIGHTS

- Various S–$CO_2$ cycles were compared in terms of application to a MCFC bottoming cycle.
- A novel concept of S–$CO_2$ cycle is proposed and intensively studied.
- The relationship of the size to the performance is studied for various S–$CO_2$ cycles.

## ARTICLE INFO

*Article history:*
Received 27 May 2014
Received in revised form
17 July 2014
Accepted 20 July 2014
Available online 30 July 2014

*Keywords:*
MCFC
S–$CO_2$ cycle
Hybrid system
PCHE

## ABSTRACT

Various supercritical carbon dioxide (S–$CO_2$) cycles for a power conversion system of a Molten Carbonate Fuel Cell (MCFC) hybrid system are studied in this paper. Re-Compressing Brayton (RCB) cycle, Simple Recuperated Brayton (SRB) cycle and Simple Recuperated Transcritical (SRT) cycle layouts were selected as candidates for this study. In addition, a novel concept of S–$CO_2$ cycle which combines Brayton cycle and Rankine cycle is proposed and intensively studied with other S–$CO_2$ layouts. A parametric study is performed to optimize the total system to be compact and to achieve wider operating range. Performances of each S–$CO_2$ cycle are compared in terms of the thermal efficiency, net electricity of the MCFC hybrid system and approximate total volumes of each S–$CO_2$ cycle. As a result, performance and total physical size of S–$CO_2$ cycle can be better understood for MCFC S–$CO_2$ hybrid system and especially, newly suggested S–$CO_2$ cycle shows some success.



## 1. Introduction

The supercritical carbon dioxide (S–$CO_2$) Brayton cycle is receiving significant attention as a promising future power conversion system due to its high efficiency under moderate operating temperature range (450–750 °C) and compact size [1]. The main reason why these advantages exist is because the S–$CO_2$ Brayton cycle has lower compressing work than other Brayton cycles due to its high density and low compressibility near the critical point where it is being compressed. Furthermore, $CO_2$ has less problems with structure material than water does which can be eventually facilitated to reach higher turbine inlet temperature with less material issues than a steam Rankine cycle [1]. Moreover, unlike the steam Rankine cycle, the chemistry control and component cooling systems are relatively simple for the S–$CO_2$ Brayton cycle, which enables the total system footprint to be greatly reduced.

The high temperature fuel cells such as molten carbonate fuel cells (MCFCs) and solid oxide fuel cells (SOFCs) are being considered as one of the next generation electric power sources because of its eco-friendliness and high efficiency advantages. The high temperature fuel cells can achieve high efficiency due to its high operating temperature and this high operating temperature is followed by high temperature exhaust heat which can be utilized as another heat source for other power conversion systems. Therefore, hybrid systems such as high temperature fuel cells coupled to gas turbine systems have been considered in the previous works [2–4]. Furthermore, since a MCFC operates at temperature range of 600–700 °C, which matches well with the operating temperature range of a S–$CO_2$ Brayton cycle, the S–$CO_2$ Brayton cycle was applied to MCFCs as a bottoming cycle to improve the total system performance previously [5,6] in addition to the gas turbine coupling study.

* Corresponding author.
*E-mail addresses:* seongjunbae@kaist.ac.kr (S.J. Bae), yoonhan.ahn@gmail.com (Y. Ahn), leejaeky85@kaist.ac.kr (J. Lee), jeongiklee@kaist.ac.kr (J.I. Lee).

http://dx.doi.org/10.1016/j.jpowsour.2014.07.121
0378-7753/

It is theoretically demonstrated that the S–$CO_2$ Brayton cycle can be a more efficient bottoming cycle for the MCFC hybrid system than the air gas turbine system for the same layout with Simple Recuperated Brayton (SRB) cycle [6]. However, various layouts were recently developed for the S–$CO_2$ cycle but applying these recent layouts to the MCFC system as a bottoming cycle was not extensively investigated. Therefore, in this paper, various S–$CO_2$ cycles are studied by changing the design conditions such as heat exchanger effectiveness to understand and compare each S–$CO_2$ cycle performance and size variation under the same boundary condition which represents the MCFC waste heat condition. Along with the SRB cycle, a Simple Recuperated Trans-critical (SRT) cycle, which has an equal number of components with the SRB cycle but having a phase change at heat emission section, is selected for this study. The Re-Compressing Brayton (RCB) cycle layout is also considered, which is widely known as the most efficient S–$CO_2$ Brayton cycle layout [1]. Additionally, in this study, authors are suggesting a novel concept of S–$CO_2$ cycle, a cascading cycle of S–$CO_2$ Brayton cycle with carbon dioxide ($CO_2$) trans-critical Rankine cycle. This S–$CO_2$ Brayton and Rankine Cascading (BRC) cycle concept is using the waste heat of the S–$CO_2$ Brayton cycle as a heat input to the $CO_2$ Rankine cycle. It was expected that by dividing the thermal power of the heat source into the Brayton cycle and the Rankine cycle of the S–$CO_2$ BRC cycle appropriately, the net system performance and operating range can be improved.

Preliminary studies of comparing performance of various S–$CO_2$ cycles will be presented when each cycle is coupled to the MCFC system. Moreover, by sizing the total heat exchanger volume, the relationship of the cycle size to the cycle performance will become apparent as well. The study is conducted by utilizing in-house codes built by KAIST research team.

## 2. Review of previous studies

Generally, a MCFC is consisted with two porous electrodes and an electrolyte which is located between each electrode, anode and cathode. Fig. 1 shows the basic principle of a MCFC, which is reproduced from Ref. [2]. First, hydrogen rich fuel feeds into the anode side and then it splits into protons and electrons. In case of electrons, they are not permitted to go through the electrolyte, so negatively charged electrons are transported to cathode side via external circuit. This electrical current generates electricity in MCFC. Oxygen from air and carbon dioxide from the anode side are fed to the cathode side while electrons from the anode side are also transported. In this reaction, a carbonate ion is formed and goes through the electrolyte to the anode side. The negatively charged carbonate ions have a chemical reaction with the protons at the anode side; eventually it maintains the charge balance and produces by-products, water and carbon dioxide. The carbon dioxide goes to the cathode as mentioned before and then the water is exhausted with heat, which the waste heat can be utilized as a heat source for other bottoming cycles [2]. This net process is only possible when the electrolyte is operated under sufficiently high temperature range, i.e. above 600 °C [3].

The high temperature fuel cell and gas turbine cycle system can be categorized into two main types, direct and indirect systems. In the case of the direct hybrid system, the air for cathode side is pressurized by compressor and the exhaust gases of the high temperature fuel cell are integrated with an open cycle gas turbine. The indirect hybrid system can be composed with open or closed power conversion cycle. Therefore, the waste heat from the exhaust gas of fuel cell is transferred through a heat exchanger [4]. The concept of such system was studied by various researchers previously [2–6]. In case of the S–$CO_2$ closed Brayton cycle, the indirect type system is generally utilized due to pressure difference between the fuel cell side and the bottoming cycle side. To investigate the S–$CO_2$ closed Brayton cycle design, an in-house code, KAIST-CCD, is developed by KAIST research team. The code is based on MATLAB and the fluid property database is from the NIST database.

In this study, the authors referred to the previous study of the MCFC operating condition [6] for the MCFC and S–$CO_2$ Brayton cycle hybrid system study. Table 1 shows the verification of the in-house code by summarizing the results from both in-house code and Ref. [6]. In Table 1, the reference values are numerical results, which were calculated under the assumed conditions in the previous research. The calculated results from the in-house code show reasonable agreement with the reference value. The same conditions will be assumed in the following analyses.

## 3. S–$CO_2$ cycle review

The S–$CO_2$ Brayton cycle is considered as one of the most attractive candidates of the waste heat recovery system due to its two notable advantages; one is its relatively high thermal efficiency

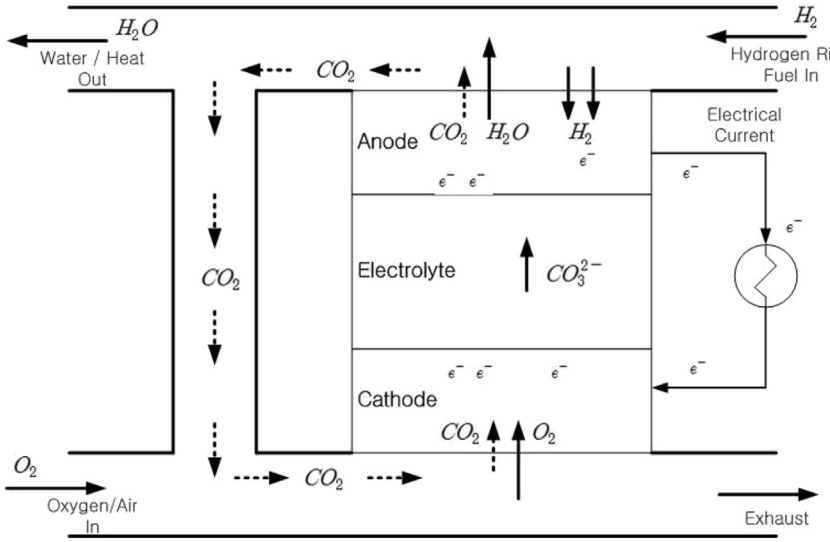


**Fig. 1.** Basic principle of a MCFC reproduced from Ref. [2].

**Table 1**
The validation of the cycle design code [6].

| | Reference value | Calculated value | Error |
|---|---|---|---|
| *MCFC* | | | |
| Current density (A $m^{-2}$) | 1100 | | |
| Area ($m^2$) | 650 | | |
| Pressure/temperature (bar/K) | 1/923 | | |
| $U_f$ (%) | 75 | | |
| $U_{CO2}$ (%) | 70 | | |
| Efficiency (%) | 50.5 | | |
| Power (kW) | 453.72 | | |
| *S–$CO_2$ SRB[a] cycle* | | | |
| Efficiency (%) | 39.9 | 39.6 | 0.8% |
| Power (kW) | 129.9 | 129.1 | 0.6% |
| *MCFC and S–$CO_2$ SRB cycle hybrid system* | | | |
| Net efficiency (%) | 59.4 | 59.3 | 0.2% |
| Net power (kW) | 583.6 | 582.8 | 0.1% |

[a] SRB: Simple Recuperated Brayton.

under the moderate temperature region and the other is inherent compactness of the whole cycle. The reason why the S–$CO_2$ Brayton cycle obtains high thermal efficiency is because it has both advantages of Brayton cycle which can achieve high turbine work at high temperature and Rankine cycle which needs small compressing power. In case of the $CO_2$, it becomes more of an incompressible fluid near the critical point resulting in low compression work. Therefore, the S–$CO_2$ Brayton cycle is usually utilized as a power cycle system for nuclear power plants, concentrated solar power systems, coal-fired plants and so on [7]. The S–$CO_2$ Brayton cycle is characterized as a highly recuperated cycle which means that the cycle requires a highly effective recuperator (i.e., a large volume of $CO_2$ to $CO_2$ heat exchanger) for minimizing heat rejection at the cooler to achieve high thermal efficiency. Furthermore, the optimized layout for high thermal efficiency could restrict $CO_2$ temperature rise in the heat receiving section [8]; which reduces the flexibility of applying the cycle for various working conditions of MCFC.

One of the well-known heat recovery systems is an Organic Rankine Cycle (ORC). It is potentially feasible application for waste heat recovery from gas turbine systems, industrial plants, geothermal resources and so on [9]. However, the $CO_2$ Rankine cycle can be very competing cycle to ORC in terms of converting low-grade waste heat into useful work because the temperature variation of $CO_2$ Rankine cycle between heat source and working fluid is better than that of the other Rankine cycles [10]. Since the $CO_2$ Rankine cycle experiences phase change, the minimum temperature of the $CO_2$ Rankine cycle is determined by the cycle minimum pressure and the $CO_2$ quality at the pump inlet. Moreover, the cycle maximum temperature of the $CO_2$ Rankine cycle for heat recovery are influenced by the heat source while the minimum temperature and pressure are set to target values.

For this study, four S–$CO_2$ cycle layouts were compared to each other while different heat exchanger effectiveness was considered. Four cycles are: The S–$CO_2$ Brayton and Rankine Cascading (BRC) cycle, Re-Compressing Brayton (RCB) cycle, Simple Recuperated Transcritical (SRT) cycle and Simple Recuperated Brayton (SRB) cycle. Each simplified cycle layout is represented in Fig. 2. The S–$CO_2$ BRC cycle is newly proposed S–$CO_2$ cycle in this study, this cycle has two S–$CO_2$ layouts thermodynamically linked to improve the system performance by appropriately using the waste heat of MCFC at each cycle. Since the S–$CO_2$ BRC and SRT cycles experience phase change of $CO_2$ at low temperature and low pressure part of the cycle, a pump and a condenser are required unlike the other S–$CO_2$ Brayton cycles used in this study. Therefore, different types of pressurizing turbomachinery and heat exchanger are required for both transcritical cycles. The

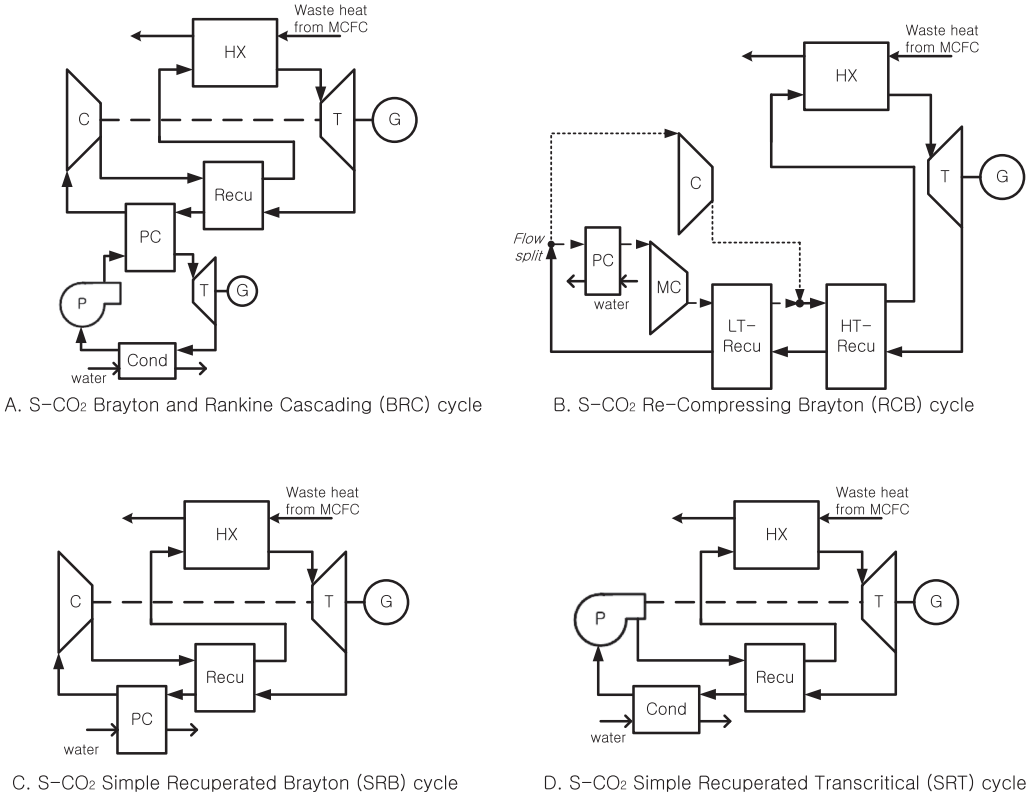


A. S–$CO_2$ Brayton and Rankine Cascading (BRC) cycle

B. S–$CO_2$ Re-Compressing Brayton (RCB) cycle

C. S–$CO_2$ Simple Recuperated Brayton (SRB) cycle

D. S–$CO_2$ Simple Recuperated Transcritical (SRT) cycle

**Fig. 2.** Various S–$CO_2$ cycle layouts studied for this study as a bottoming cycle for the MCFC hybrid system.

uniqueness of the S–$CO_2$ RCB cycle compared to other cycles is that some portion of $CO_2$ flow is split and compressed separately to avoid pinch-point issues in the recuperator as well as to improve net system performance.

Fig. 3 shows the configuration of S–$CO_2$ BRC cycle in more detail. The S–$CO_2$ BRC cycle is using the two cycle configurations; the simple recuperated Brayton cycle and the simple Rankine cycle. The Brayton cycle part of the S–$CO_2$ BRC cycle is connected with the main heat source (i.e. MCFC). The Rankine cycle is connected to the Brayton cycle via pre-cooler to use the waste heat of the Brayton cycle as a heat input. Since the exhaust heat of general S–$CO_2$ Brayton cycle is rejected to the ultimate heat sink, by utilizing the heat via $CO_2$ Rankine cycle, the net system efficiency can be improved, and the recuperator in the Brayton cycle does not need to have high effectiveness; eventually the volume of the recuperator can be reduced while maintaining high performance.

Even though each cycle of the S–$CO_2$ BRC cycle is physically independent, it is thermodynamically linked. Therefore, since the cycle operating conditions of each Brayton cycle and Rankine cycle affect each cycle performance, the S–$CO_2$ BRC cycle design parameters including pressure ratio, minimum temperature and others were optimized. The *T*–*S* diagram including the Brayton and Rankine cycles for the S–$CO_2$ BRC cycle is shown in Fig. 4. The reason why $CO_2$ Rankine cycle is considered for additional cycle for this S–$CO_2$ BRC cycle is because $CO_2$ Rankine cycle can achieve high thermal efficiency with relatively low temperature operating range, therefore the $CO_2$ Rankine cycle can effectively use the waste heat of S–$CO_2$ Brayton cycle.

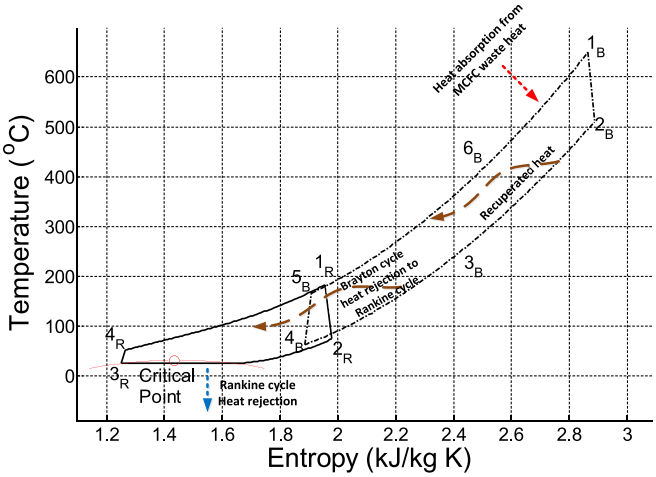


**Fig. 4.** *T*–*S* diagram of the S–$CO_2$ BRC cycle.

The S–$CO_2$ RCB cycle utilizes two recuperators and two compressors as shown in Fig. 5. The RCB cycle is known as one of the most efficient layouts for the S–$CO_2$ Brayton cycle [1]. Reducing the waste heat and increasing the recuperated heat by recompressing some portion of the flow is the main concept of the RCB cycle to increase the cycle thermal efficiency [11]. The *T*–*S* diagram of the S–$CO_2$ RCB cycle is shown in Fig. 6. In this case, the main compressor inlet condition should be near the critical point of $CO_2$ to reduce the main compressor work. The S–$CO_2$ RCB cycle can

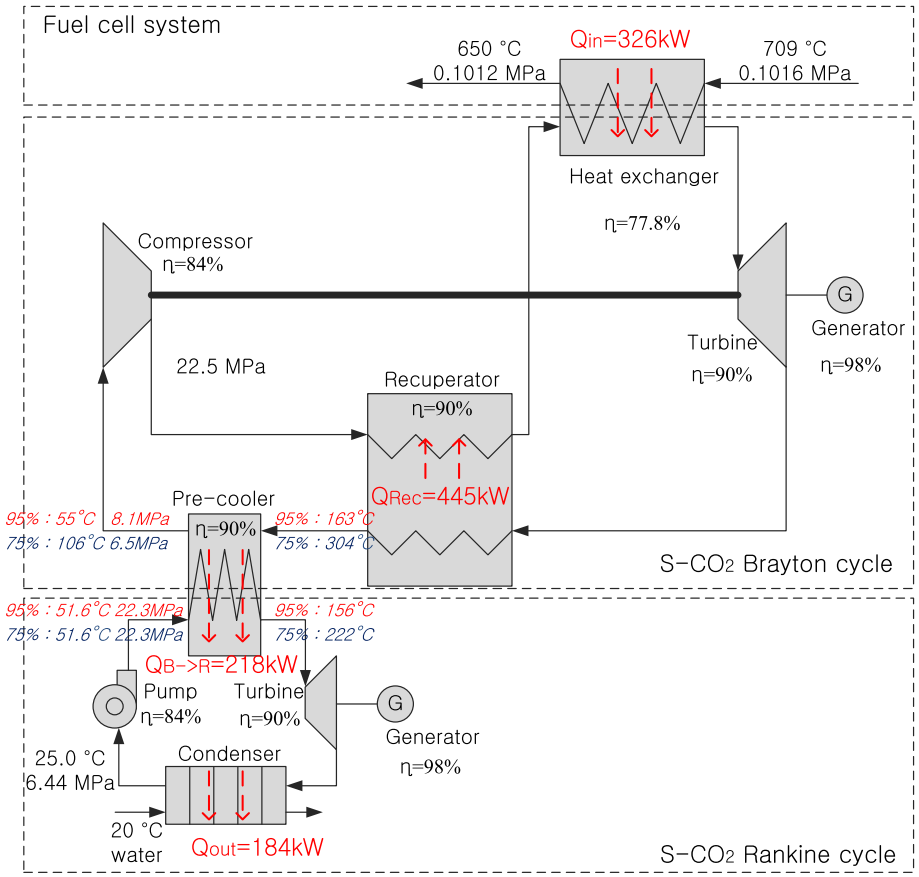


**Fig. 3.** S–$CO_2$ Brayton and Rankine Cascading (BRC) cycle operating conditions for 75% and 95% heat exchanger effectiveness cases.

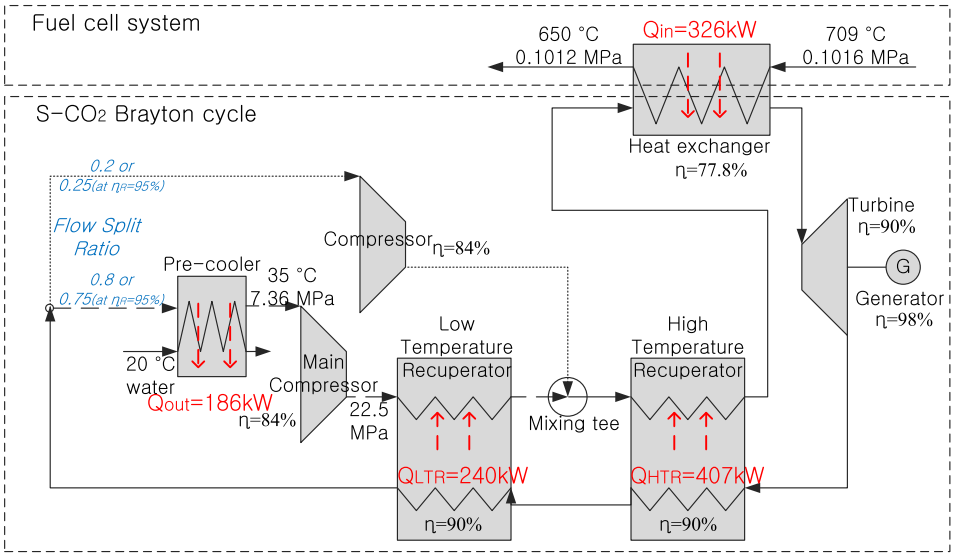


**Fig. 5.** S–$CO_2$ Re-Compressing Brayton (RCB) cycle operating conditions.

achieve high cycle efficiency due to low waste heat by using two recuperators. However, two recuperators occupy nearly the whole physical volume of the cycle as it will be demonstrated in the following study as well as shown in the previous studies [1].

Since, even the SRB cycle layout is considered as a good option for small and medium size system due to its simple configuration and reasonable thermal efficiency, the S–$CO_2$ SRB cycle and the S–$CO_2$ SRT cycle are evaluated in this study as reference cases. Figs. 7 and 8 show each cycle layout, respectively. Both cycle configurations are similar with the cycle layout used in the previous studies [6]. In case of the S–$CO_2$ SRB cycle, the compressor inlet temperature is assumed to be 35 °C so that it is close to the critical point of $CO_2$. Whereas the minimum temperature of the S–$CO_2$ SRT cycle is assumed to be 25 °C, and this is under the critical temperature of $CO_2$ (i.e. liquid phase). This minimum temperature of the S–$CO_2$ SRT cycle was determined while the bottom cycle minimum temperature of the S–$CO_2$ BRC cycle was determined as well. Therefore, the S–$CO_2$ SRT cycle has a pump and a condenser instead of a compressor and a pre-cooler unlike the SRB cycle. Although configurations of both SRB and SRT cycles are very similar, the operating condition of pressurizing turbomachinery is at supercritical state for SRB (i.e. compressor) and it is in liquid phase for SRT (i.e. pump). In case of pump, the quality of working fluid at pump inlet is a significant factor for designing turbomachinery. In other words the low pressure and low temperature section of the two cycles are very different and therefore, even though the layouts are similar to each other they should be considered as two separate power cycles. The *T*–*S* diagrams of the S–$CO_2$ SRB cycle and SRT cycle are presented in Figs. 9 and 10, respectively. These *T*–*S* diagrams roughly show that the pumping (or compressing) work of the S–$CO_2$ SRT cycle is lower than that of the S–$CO_2$ SRB cycle.

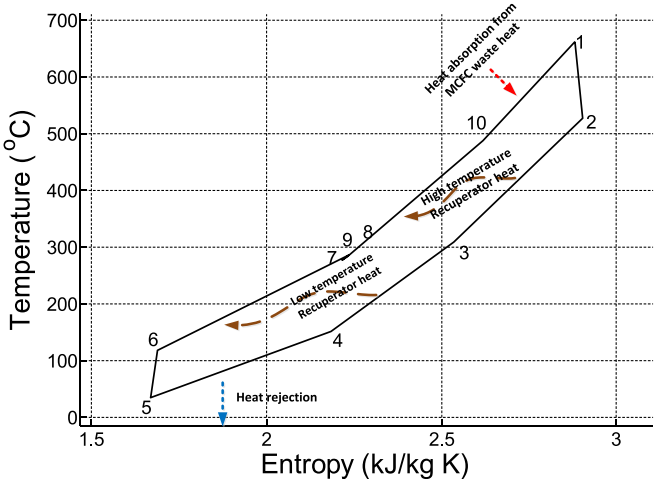


**Fig. 6.** *T*–*S* diagram of the S–$CO_2$ RCB cycle.

## 4. Cycle performance evaluation

The cycle performances including thermal efficiency and net electricity of the selected S–$CO_2$ cycles were calculated while the heat exchanger effectiveness was being varied under the MCFC operating conditions. Basic parameters including the heat input from the MCFC, cycle maximum pressure and performance of components such as turbomachinery efficiency and heat exchanger effectiveness were referred from the previous research work [6]. In case of the S–$CO_2$ RCB cycle, it is assumed that the effectiveness of both recuperators are the same. It is noted that the RCB cycle is required to find the optimum flow split ratio between the total flow and the main compressor flow when cycle design condition changes. In this study, the optimum flow split ratio (i.e. ratio between the main compressor flow and the total flow) is defined as a value which makes the S–$CO_2$ RCB cycle to achieve the highest thermal efficiency. Fig. 11 shows the optimum flow split ratio for the assumed recuperator effectiveness. As the result clearly demonstrates that 0.8 flow split ratio is optimal for the RCB cycle with recuperators below 90% effectiveness while 0.75 flow split ratio is the optimum for the cycle with recuperators over 95% effectiveness.

To compare each S–$CO_2$ cycle performance under the assumed parameters, the optimized pressure ratio should be also studied when the cycle design conditions change. Since the compressor of both S–$CO_2$ RCB and S–$CO_2$ SRB cycles operate near the critical point of $CO_2$, the cycle minimum temperature and pressure were fixed to 35 °C and 7.5 MPa based on the reference [6]. However, since the minimum temperature of the S–$CO_2$ SRT cycle has to be

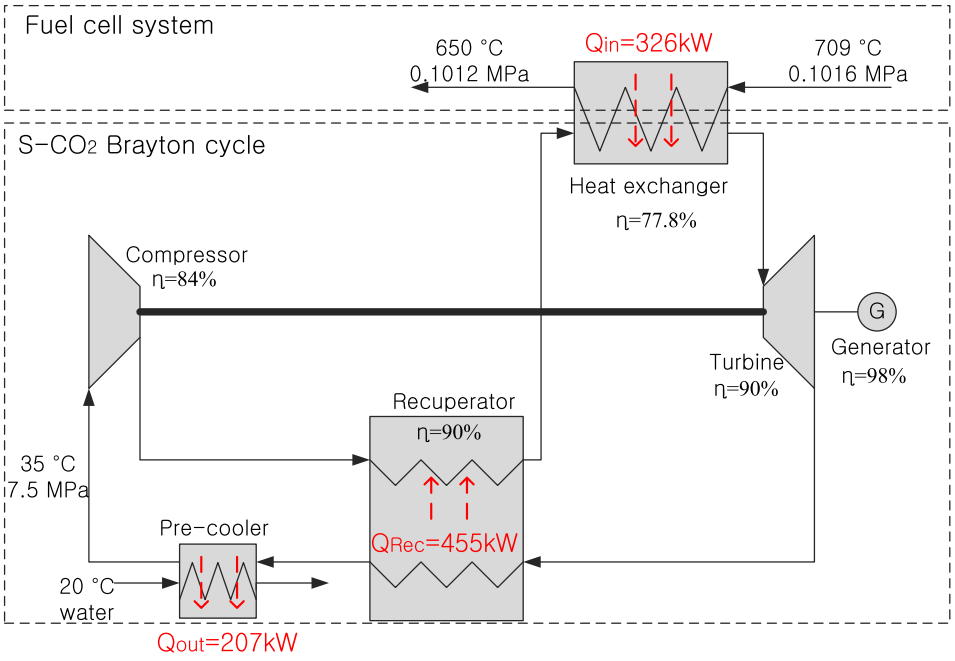


**Fig. 7.** S–$CO_2$ Simple Recuperated Brayton (SRB) cycle operating conditions.

below the critical temperature, 25 °C was assumed. Thus, the minimum pressure should be 6.43 MPa (i.e. Saturation pressure at 25 °C) whereas the cycle maximum pressure is equally at 22.5 MPa. In this study, to simplify the cycle analysis, the pump inlet condition of the S–$CO_2$ SRT cycle is assumed as saturated liquid condition; the quality of $CO_2$ is zero at pump inlet.

However, in case of the S–$CO_2$ BRC cycle, the pressure ratio which enables the cycle to produce the most electricity should be chosen for both Brayton and Rankine cycles. Moreover, the pressure ratios of the S–$CO_2$ BRC cycle are affected by not only the effectiveness of heat exchangers but also the Compressor Inlet Temperature (C.I.T) of the Brayton cycle side. Therefore, the pressure ratio of each cycle consisting the S–$CO_2$ BRC cycle was studied.

Similar to the S–$CO_2$ SRT cycle, the pump inlet condition of the S–$CO_2$ BRC cycle Rankine side is assumed at saturated liquid state to simplify the cycle analysis; the quality of $CO_2$ is zero at the pump inlet. As a result, the cycle minimum pressure of the S–$CO_2$ BRC cycle Rankine side is selected to be around 6.43 MPa to achieve the target cycle minimum temperature, 25 °C. Figs. 12 and 13 show the results of the optimum pressure ratios, which each cycle can achieve the highest thermal efficiency under the given heat exchanger effectiveness and the C.I.T of the Brayton cycle side. It is assumed

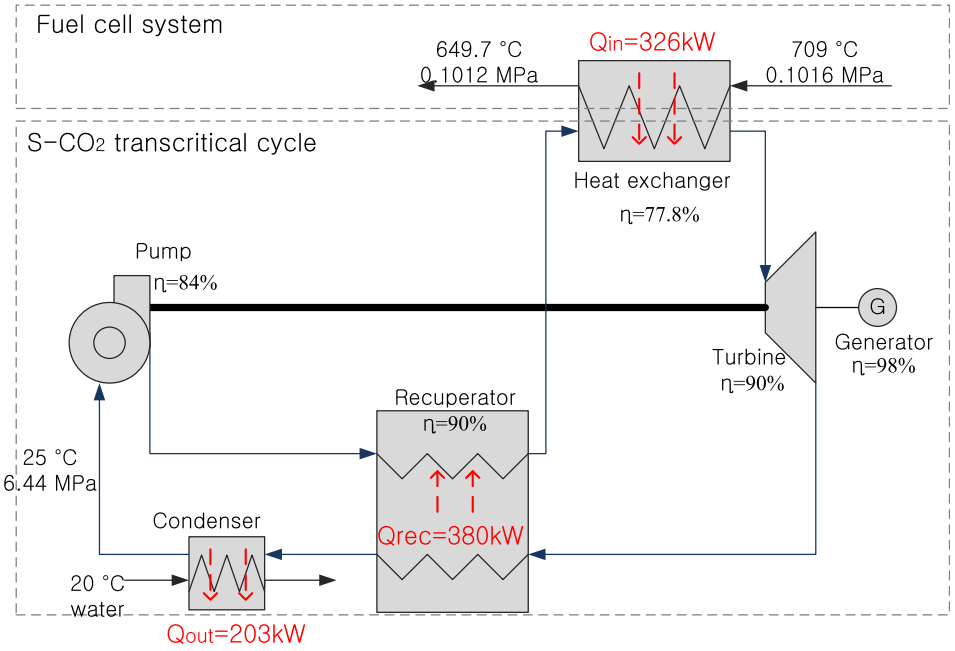


**Fig. 8.** S–$CO_2$ Simple Recuperated Transcritical (SRT) cycle operating conditions.

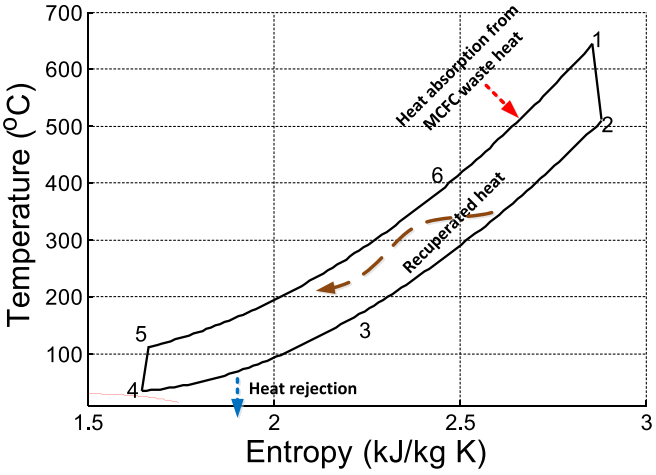


**Fig. 9.** *T–S* diagram of the S–$CO_2$ SRB cycle.

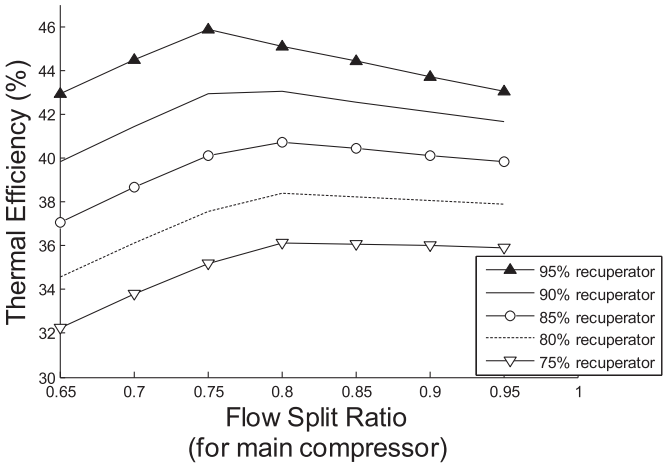


**Fig. 11.** The flow split ratio study for different recuperator effectiveness under the S–$CO_2$ RCB cycle operating conditions.

that the pre-cooler effectiveness of the S–$CO_2$ BRC cycle is the same with the recuperator effectiveness. In case of the S–$CO_2$ BRC cycle Rankine side, since the cycle minimum pressure is fixed around 6.43 MPa (i.e. saturation pressure of $CO_2$ at 25 °C), the cycle maximum pressure of the Rankine cycle side can be simultaneously obtained through the pressure ratio study as summarized in Fig. 13. Collecting the results of the pressure ratio studies of the S–$CO_2$ BRC cycle, the net produced electricity of the S–$CO_2$ BRC cycle is shown in Fig. 14 for various C.I.T and heat exchanger effectiveness. To normalize the net produced power of the S–$CO_2$ BRC cycle, the value is determined as the ratio of the net power of MCFC hybrid system adopting the S–$CO_2$ BRC cycle to the net power of MCFC alone system. Fig. 14 shows that each case has an optimum for maximizing the cycle performance for given heat exchanger effectiveness. However, relatively high cycle maximum pressure is needed for the Rankine cycle side of the S–$CO_2$ BRC cycle; even exceeding 40 MPa under 80% heat exchanger effectiveness cases. Such high pressures that originate from high pressure ratio of the Rankine cycle side of the S–$CO_2$ BRC cycle would be fairly difficult to realize due to many challenges associated with the high pressure system. Thus, in this study, the pressure ratio around 3.4–3.5 were selected for the Rankine cycle side of the S–$CO_2$ BRC cycle to assume reasonable design conditions. Thus the cycle maximum pressures of the Rankine cycle side is restricted to 22–23 MPa; the maximum pressure of the Rankine cycle side is similar to the value of the Brayton cycle side. The optimized design points are also shown in Figs. 13 and 14 as red circular marks (in the web version) for given heat exchanger effectiveness. It is worthwhile to mention that the difference between the performance maximizing design point (blue triangle) and the optimized design point (red circle) is gradually decreasing as the heat exchanger effectiveness increases as it is shown in both Figs. 13 and 14. For instance, for 95% effectiveness case, both design points are almost equal to each other. After including the optimized BRC cycle result, Table 2 summarizes the assumed parameters of all four S–$CO_2$ cycles coupled to a MCFC system.

Considering the previous study of each S–$CO_2$ cycle, the thermal efficiency of the S–$CO_2$ cycles and net system power ratio (i.e. generated power ratio between the MCFC & S–$CO_2$ cycle hybrid system and the MCFC alone system) are calculated for various heat exchanger effectiveness as shown in Figs. 15 and 16, respectively. In case of the S–$CO_2$ BRC cycle, both high pressure design and optimal pressure design cases are shown, respectively in the figure.

As shown in the results, the performance of the S–$CO_2$ BRC cycle is higher than that of the other S–$CO_2$ cycles, except for the case

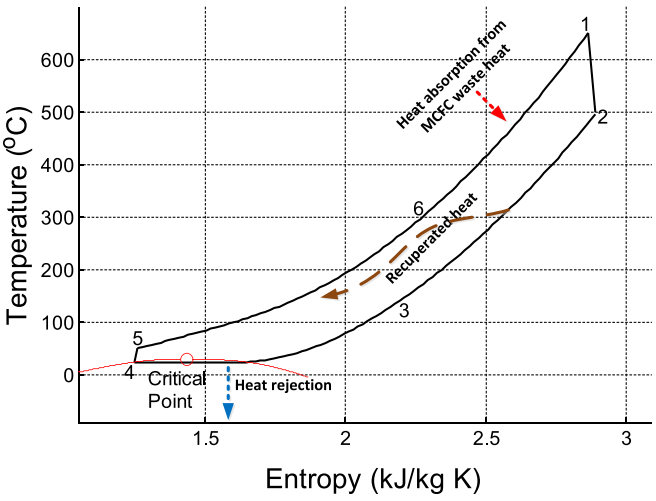


**Fig. 10.** *T–S* diagram of the S–$CO_2$ SRT cycle.

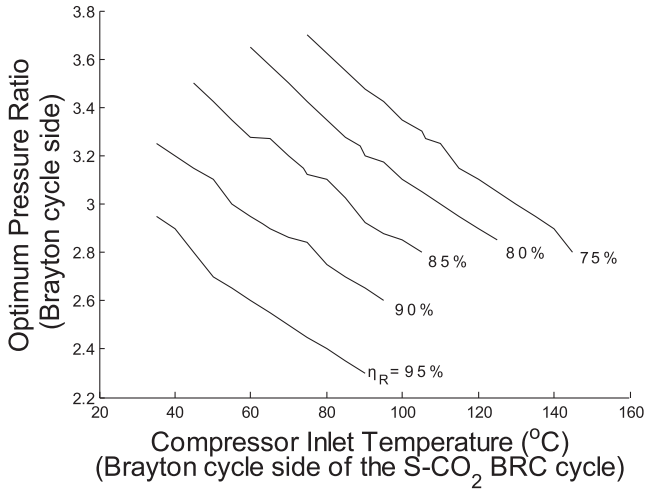


**Fig. 12.** The Brayton cycle side pressure ratio study for different C.I.T and heat exchanger effectiveness under of the S–$CO_2$ BRC cycle operating conditions.

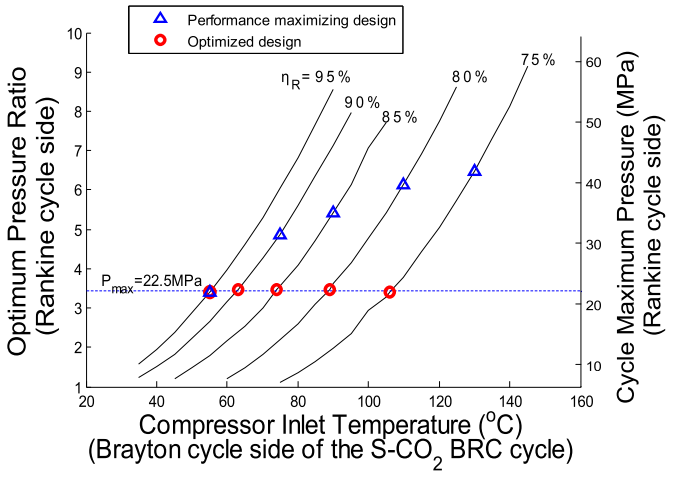


**Fig. 13.** The Rankine cycle side pressure ratio study for different C.I.T and heat exchanger effectiveness under the S–$CO_2$ BRC cycle operating conditions.

with low heat exchanger effectiveness. In case of the S–$CO_2$ RCB cycle, the performance is almost similar to the S–$CO_2$ BRC cycle; even higher at relatively low heat exchanger effectiveness range. The S–$CO_2$ SRT cycle and S–$CO_2$ SRB cycle show similar trend. Table 3 summarizes the results of various MCFC and S–$CO_2$ cycle hybrid systems studied in this paper for 95% heat exchanger effectiveness condition, and the air Brayton cycle MCFC hybrid system is also shown [6]. This result indicates that the S–$CO_2$ cycle can be very competitive to an air Brayton cycle in terms of the cycle performance; even in case of the S–$CO_2$ BRC and RCB cycles, the net efficiency improvement of hybrid system can be more than 10% in comparison to the MCFC alone system.

To compare each cycle more reasonably a specific power, the ratio of the generated power to the $CO_2$ mass flow rate, is compared for each S–$CO_2$ cycle. The specific power is related to the pressure loss, pipe selection and eventually price competitiveness of the cycle. Fig. 17 represents the specific power comparison while heat exchanger effectiveness was being varied. In case of the S–$CO_2$ BRC cycle, the specific power is separately represented for each cycle, the Brayton cycle side and Rankine cycle side, because both cycles are physically independent.

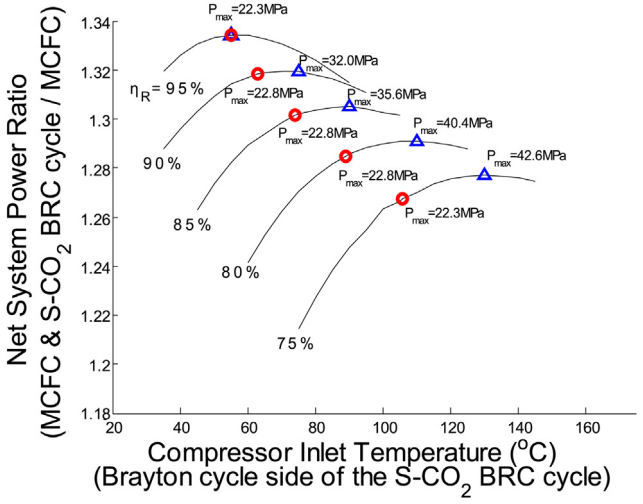


**Fig. 14.** The S–$CO_2$ BRC cycle net power generation study for various C.I.T and heat exchanger effectiveness.

**Table 2**
Assumed parameters of each S–$CO_2$ cycle [6].

| Parameter | SRB cycle | SRT cycle | RCB cycle | BRC cycle | |
|---|---|---|---|---|---|
| | | | | (Brayton) | (Rankine) |
| $Q_{MCFC}$ (kWth) | 326 | | | 326 | |
| $P_{max}$ (MPa) | 22.5 | | | 22.5 | 22–23 |
| $T_{min}$ (°C) | 35 | 25 | 35 | – | 25 |
| PR | 2.85 | 3.31 | 2.77 | – | 3.4–3.5 |
| $\eta_T$ (%) | 90 | | | 90 | 90 |
| $\eta_C$ (%) | 84 | | | 84 | 84 |
| $\eta_R$ (%) | 75–95 | | | 75–95 | None |

In cases of the SRT, SRB and RCB cycles, the specific power values change very similarly with heat exchanger effectiveness. The reason is because as the recuperator effectiveness improves, less temperature difference is obtained at the heat exchanger for recovering MCFC waste heat, which eventually leads to high mass flow rate as well as high cycle performance. Whereas, the S–$CO_2$ SRT cycle mass flow rate is relatively low due to its large temperature difference at the heat receiving section originated from the low cycle minimum temperature which is under the critical point of $CO_2$. Therefore, the specific power of the S–$CO_2$ SRT cycle is higher than that of the other S–$CO_2$ cycles used in this paper.

On the other hand, in cases of the S–$CO_2$ BRC cycle specific power, a significant variation is observed compared to the other S–$CO_2$ cycle cases. Since both cycles consisting the S–$CO_2$ BRC cycle, the Brayton cycle and the Rankine cycle, are designed to achieve the highest efficiency, the specific power value of each Brayton cycle and Rankine cycle in the S–$CO_2$ BRC cycle is lower than that of other S–$CO_2$ cycles.

The analysis of the total hybrid system net performance was carried out while the MCFC side heat exchanger outlet temperature is being changed. The result is shown in Fig. 18. It is noted that the heat exchanger effectiveness was fixed at 90% while other parameters were assumed to be the same. The results show gradual increase of the net power while the hot side outlet temperature decreases for all S–$CO_2$ cycle layouts. Within the considered temperature range, the S–$CO_2$ BRC cycle shows a good performance, but it is also very close to the S–$CO_2$ RCB cycle performance as well. The temperature of the MCFC waste heat side needs to be above the operating temperature of a MCFC to minimize the effect on MCFC side, therefore 600 °C was chosen for the lower limit of the temperature in this study.

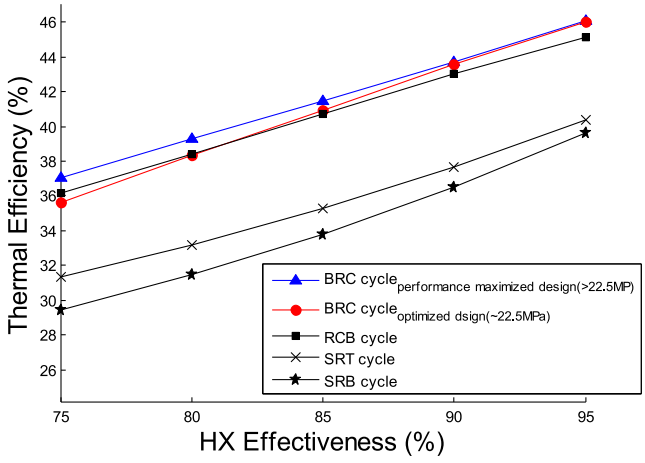


**Fig. 15.** The thermal efficiency vs. heat exchanger effectiveness for various layouts.

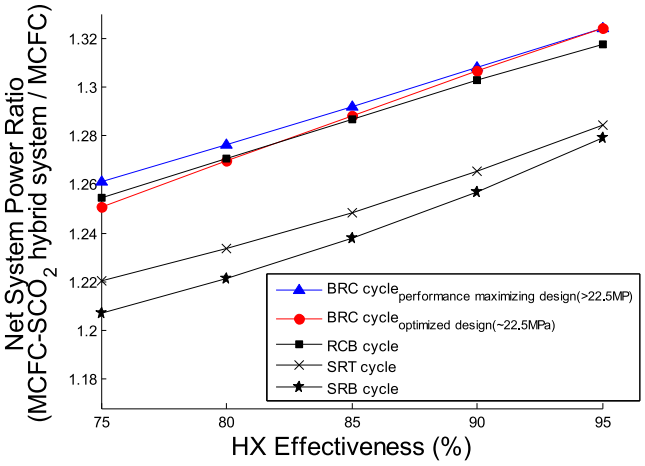


**Fig. 16.** The MCFC with S–$CO_2$ cycle system net power ratio vs. heat exchanger effectiveness for various layouts.

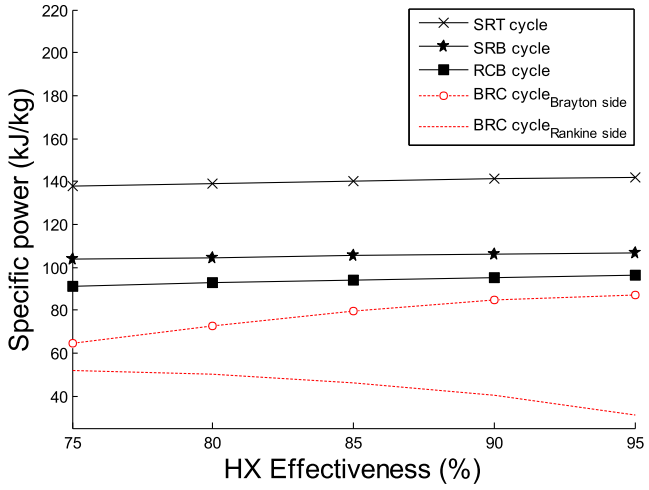


**Fig. 17.** The specific power vs. heat exchanger effectiveness for various layouts.

## 5. Comparison of the total heat exchanger volume of each S–$CO_2$ cycle

Sine the MCFC hybrid system can be utilized as a distributed power generation system, transportability can be an important issue. Therefore, minimizing total MCFC hybrid system volume can be one of the major design requirements. As mentioned above, one advantage of the S–$CO_2$ cycle is that it can have compact configuration due to its small components and simple layout [1,12,13]. However, since turbomachinery of the S–$CO_2$ cycle is very small compared to the volume of heat exchangers [1,13], the size estimation of the S–$CO_2$ cycle is directly connected to the heat exchanger design. Therefore, from the previous cycle analysis results, the total heat exchanger volume which includes recuperators and pre-cooler or condenser can be evaluated and compared for different cycles while the heat exchanger effectiveness are being varied.

Heat exchanger design was carried out by assuming that water is the pre-cooler or the condenser cold side coolant acting as an ultimate heat sink. The material of the heat exchanger was selected to be AISI 316 and all heat exchangers were assumed to be the Printed Circuit Heat Exchanger (PCHE) type. The reason is because not only the PCHE has high surface to volume density but also it has a wide operating range of pressure and temperature up to 40 MPa and 900 °C [14]. An in-house PHCE design code, KAIST-HXD developed by the KAIST research team, is utilized to design the PCHE for the S–$CO_2$ cycles. The KAIST-HXD is based on MATLAB and the fluid property database is adopted from the NIST database. The KAIST-HXD assumes the PCHE flow configuration as a counter current flow heat exchanger and calculates the optimal design conditions to obtain the minimum volume that meets the target effectiveness and pressure drop requirement. However, the in-house code is restricted to design the PHCE main body only, so other parts such as headers, ducts, and etc. are neglected from the size estimation.

Fig. 19 shows the results of the estimated total volume of heat exchangers of each S–$CO_2$ cycle. To compare each S–$CO_2$ cycle volume in a normalized form, the total heat exchanger volume of each case is divided by the volume of SRB cycle with 95% heat exchanger effectiveness case. As shown in the figure, the total heat exchanger volume of the S–$CO_2$ BRC cycle and S–$CO_2$ RCB cycle are higher than those of the other cycles as expected. Each heat exchanger volume of investigated S–$CO_2$ cycles is summarized in Table 4 for 75, 85 and 95% heat exchanger effectiveness cases. As show in Table 4, since the S–$CO_2$ RCB cycle is designed to reduce the waste heat and increase the recuperated heat as much as possible, it has large recuperators than other S–$CO_2$ cycles. However, Table 4 also shows that the S–$CO_2$ BRC cycle pre-cooler is larger than that of the other S–$CO_2$ cycles. This is because the pre-cooler of the S–$CO_2$ BRC cycle functions as a

**Table 3**
Various MCFC hybrid system performance comparison [6].

| | | | | | |
|---|---|---|---|---|---|
| *MCFC* | | | | | |
| Efficiency (%) | 50.5 | | | | |
| Power (kW) | 453.72 | | | | |
| *Bottoming cycle* | | | | | |
| Coolant | $CO_2$ | | | | Air |
| Layout | SRB | SRT | RCB | BRC | SRB |
| Efficiency (%) | 39.6 | 40.4 | 45.1 | 46.1 | 26.6 |
| Power (kW) | 129.1 | 131.7 | 147.1 | 150.1 | 86.7 |
| *MCFC and bottoming cycle hybrid system* | | | | | |
| Net efficiency (%) | 59.3 | 59.6 | 61.1 | 61.5 | 55 |
| Net power (kW) | 582.8 | 585.4 | 600.8 | 603.8 | 540.4 |

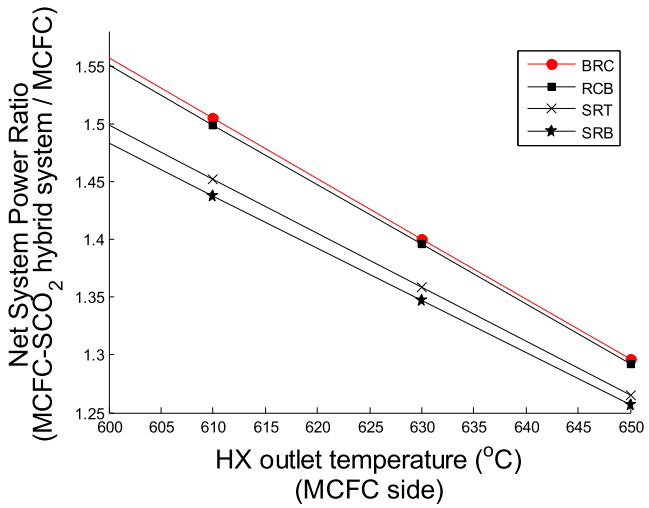


**Fig. 18.** The MCFC and S–$CO_2$ cycle hybrid system's net power ratio vs. heat exchanger outlet temperature of the MCFC side for various layouts.

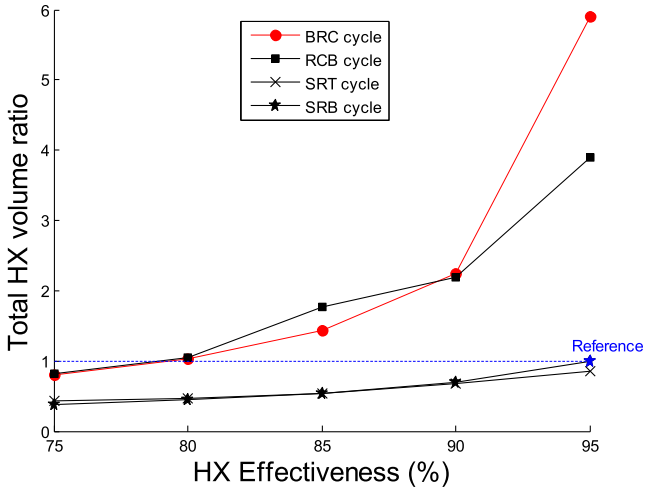


**Fig. 19.** The total heat exchanger volume ratio (i.e. ratio of the total HX volume of each case to that of SRB cycle using 95% HX) vs. heat exchanger effectiveness for various layouts.

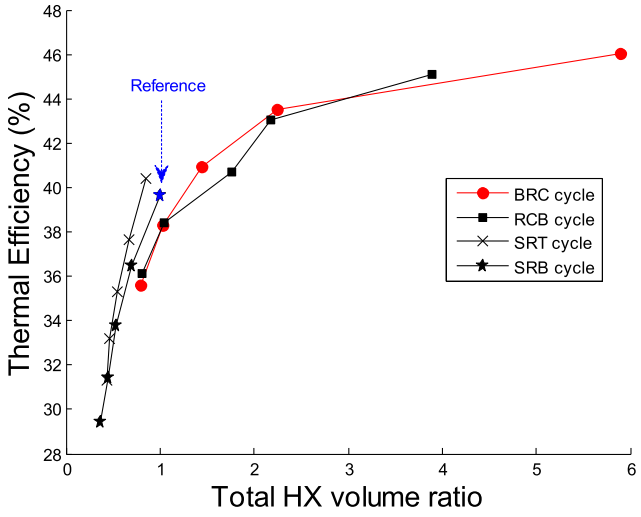


**Fig. 20.** The thermal efficiency vs. total heat exchanger volume ratio for various layouts.

cooler for the Brayton cycle side as well as a heat source for the Rankine cycle side; thus it becomes similar to the low temperature recuperator of the S–$CO_2$ RCB cycle. Fig. 19 and Table 4 show that the total heat exchanger volume of each cycle increases as the heat exchanger effectiveness becomes higher. It is noted that a sharp increase is observed for the S–$CO_2$ BRC cycle heat exchanger volume when the effectiveness is in between 90 and 95%. This is because as the heat exchanger effectiveness increases, the optimal C.I.T of the Brayton cycle side is decreasing as shown in Fig. 14; the C.I.T is the hot side outlet temperature of the S–$CO_2$ BRC cycle pre-cooler. The cold side inlet temperature is almost the same regardless of the pre-cooler effectiveness because the cycle maximum pressure of the Rankine cycle side is fixed to 22–23 MPa and the pump inlet pressure is also fixed to 6.44 MPa which is the saturation pressure at 25 °C. Fig. 3 shows the two cases of the S–$CO_2$ BRC cycle using heat exchangers with 75% and 95% effectiveness, respectively. In case of using heat exchanger with 75% effectiveness, the temperature difference between the hot side outlet temperature of the pre-cooler and the cold side inlet temperature of the pre-cooler is about 54.4 °C, whereas for 95% case, just 3.4 °C difference exists; small temperature difference between hot and cold sides will have issues for designing and manufacturing the heat exchanger.

For the S–$CO_2$ SRT cycle and the S–$CO_2$ SRB cycle, Fig. 19 shows that volume difference is not that significant for different heat exchanger effectiveness due to large temperature difference between heat exchangers. The heat exchanger volume of both S–$CO_2$ cycles is smaller than that of the S–$CO_2$ RCB cycle and S–$CO_2$ BRC cycle because simple recuperated cycle layouts have smaller number of heat exchangers than the other cycles. Moreover, since both simple recuperated cycle layouts have lower mass flow rate and higher temperature difference at the recuperator than the S–$CO_2$ BRC cycle and S–$CO_2$ RCB cycle, the recuperators of both simple recuperated Brayton and Rankine cycles would be relatively compact; eventually recuperators with smaller volume are designed as shown in Table 4. On the other hand, in case of the S–$CO_2$ SRT cycle, the volume of the condenser is higher than the pre-cooler of SRB cycle because this cycle should achieve considerably low pump inlet temperature of 25 °C from the recuperator outlet condition.

Fig. 20 shows the thermal efficiency of each S–$CO_2$ cycle while the total heat exchanger volume is changing. The total heat exchanger volume is indicated as the ratio (i.e. ratio between the total heat exchanger volume of each case and that of SRB cycle using 95% effectiveness heat exchangers) as before. This graph can be considered as a cost performance ratio because the total heat exchanger volume is related to not only the price of the heat exchanger but also the transportability of the total system as well. As show in the result, to achieve significant additional power generation by the S–$CO_2$ cycle, the S–$CO_2$ BRC cycle or the S–$CO_2$ RCB cycle can be a good option. However, in relatively low thermal efficiency range, 36–40%, all S–$CO_2$ cycle layouts are possible while having small heat exchanger volume. Especially, for the intermediate performance condition, about 40–44% efficiency range, the S–$CO_2$ BRC cycle can be a better choice over the S–$CO_2$ RCB cycle, but if the designer requires thermal efficiency higher than 44%, competitiveness of the S–$CO_2$ BRC cycle is sharply decreased due to the large pre-cooler. These results are summarized in Table 5. In this table, optimum cycle means the cycle achieving the highest performance with the same physical volume.

**Table 4**
Heat exchanger volume of S–$CO_2$ cycles.

| (Unit: $cm^3$) | $\eta_R$ (%) | Recuperator | Pre-cooler | Condenser |
|---|---|---|---|---|
| SRB cycle | 75 | 2062 | 2100 | |
| | 85 | 3742 | 2199 | |
| | 95 | 8909 | 2322 | |
| SRT cycle | 75 | 1609 | | 3226 |
| | 85 | 2846 | | 3207 |
| | 95 | 6607 | | 2989 |
| RCB cycle | 75 | 3006/3727 | 2388 | |
| | 85 | 7775/9516 | 2562 | |
| | 95 | 20,379/20,897 | 2443 | |
| BRC cycle | 75 | 2646 | 3745 | 2553 |
| | 85 | 4792 | 8246 | 3161 |
| | 95 | 11,699 | 51,770 | 2739 |

**Table 5**
Each S–$CO_2$ cycle performance and size result summery.

| Total heat exchanger volume ratio | ~1 | 1–3 | 3~ |
|---|---|---|---|
| Optimum cycle | SRT | BRC | RCB |

## 6. Conclusions

In this paper, various S–$CO_2$ cycle layouts are applied as the bottoming cycle for utilizing the waste heat of the MCFC. Since the waste heat temperature range of the MCFC corresponds well with the S–$CO_2$ cycle, and it has compact components and simple configuration, the S–$CO_2$ cycle can be a good bottoming cycle for the MCFC hybrid system. Therefore, to compare the performance of various S–$CO_2$ cycles, four cycles were selected and studied: (1) Simple Recuperated Brayton (SRB) cycle, (2) Simple Recuperated Transcritical (SRT) cycle, (3) Re-Compressing Brayton (RCB) cycle, and (4) Brayton and Rankine Cascading (BRC) cycle. Especially, the S–$CO_2$ BRC cycle is newly proposed S–$CO_2$ cycle in this study, and the characteristics of the proposed cycle were studied for the first time. This study shows that all of the analyzed S–$CO_2$ cycles are more competitive bottoming cycle for the MCFC system than the air Brayton cycle in terms of the cycle performance; for example the S–$CO_2$ BRC cycle and the S–$CO_2$ RCB cycle can increase the net hybrid system efficiency more than 10% than the single MCFC system.

The analysis results show that the S–$CO_2$ BRC cycle has some promising potential in terms of performance; thermal efficiency can be slightly higher or equal than the S–$CO_2$ RCB cycle which is known as one of the most efficient cycle layouts for S–$CO_2$ cycle previously. Especially, it was predicted that the S–$CO_2$ BRC cycle can be the most competitive layout in terms of the efficiency as well as the physical size when the available heat exchanger effectiveness is around 80–90%. However, to achieve higher efficiency by utilizing a heat exchanger with higher effectiveness than 90%, the total heat exchanger volume of the S–$CO_2$ BRC cycle increases steeply due to the rapid increase in size of the heat exchanger (i.e. precooler of the Brayton cycle) that connects the Brayton cycle and the Rankine cycle. The reason is because the connecting heat exchanger of the S–$CO_2$ BRC cycle acts as a cooler for the Brayton cycle side and a heater for the Rankine cycle side at the same time, and this function resembles the low temperature recuperator of the S–$CO_2$ RCB cycle.

Furthermore, it was predicted that if the available space for the bottoming system is restricted, the S–$CO_2$ SRT cycle shows the best performance than other S–$CO_2$ cycles analyzed in this study with similar size. The S–$CO_2$ SRT cycle can be also economical layout due to high specific power. Since the specific power is related to the pressure losses, pipe selection and capital cost of the cycle, it is one of the important factors which cycle designers should be aware of. On the contrary to the SRT cycle, the BRC cycle has relatively low specific power which can be another disadvantage of the proposed cycle. Therefore, if the BRC cycle is going to be more competitive by overcoming the specific power issue and the heat exchanger volume issue, further optimization and innovation are required for the S–$CO_2$ BRC cycle. It is shown that no single S–$CO_2$ cycle layout can be successful for wide range of design requirements. Thus the study on the selection of an appropriate cycle layout and optimization of the operating conditions are required to maximize the performance of the MCFC hybrid system.

In this study, the S–$CO_2$ cycles are designed to use the waste heat of the MCFC via a heat exchanger, thus the bottoming cycle can match the MCFC performance through re-optimization if the MCFC performance varies from the reference. However, even though the cycle can be re-optimized for different MCFC design conditions, if the operating top temperature does not change, most of the conclusions derived from this study will be still valid. This is because the cycle performance and physical size rises from the genuine characteristics of the cycle layout itself and the operating temperature mostly.

## Acknowledgments

The authors gratefully acknowledge that this research was financially supported by the National Research Foundation (NRF) and the Korean Ministry of Science, ICT and Future Planning (2012R1A1A1013968).

## Nomenclature

| | |
|---|---|
| $U_f$ | fuel utilization factor |
| $U_{CO2}$ | carbon dioxide utilization factor |
| $\eta$ | efficiency or effectiveness |
| $Q_{MCFC}$ | fuel cell waste heat |
| $P_{max}$ | cycle maximum pressure |
| $T_{min}$ | cycle minimum temperature |
| PR | turbine pressure ratio |

*Subscript*

| | |
|---|---|
| T | turbine |
| C | compressor |
| R | recuperator |

## References

[1] V. Dostal, M.J. Driscoll, P. Hejzlar, A Supercritical Carbon Dioxide Cycle for Next Generation Nuclear Reactors, 2004. MIT-ANP-TR-100.
[2] S.T. Revankar, M. Wolff, C. Gutierrez, K. Justice, B. Wolf, Islanding and Distributed Generation for Enhanced Electric Power Grid Security, 2007. PU/NE-07–16.
[3] S. Ubertini, P. Lunghi, Assessment of an Ambient Pressure MCFC: External Heated GT Hybrid Plant with Steam Injection and Post-Compustion, vol. 1, 2001, pp. 174–180.
[4] D. Sánchez, R. Chacartegui, F. Jimenéz-Espadafor, T. Sánchez, J. Fuel Cell Sci. Technol. 6 (2009) 021306.
[5] K.S. Oh, T.S. Kim, J. Power Sources 158 (2006) 455–463.
[6] D. Sánchez, J.M. Muñoz de Escalona, R. Chacartegui, A. Muñoz, T. Sánchez, J. Power Sources 196 (2010) 4347–4354.
[7] Ma Zhiwen, S. Turchi Craig, in: Advanced Supercritical Carbon Dioxide Power Cycle Configurations for Use in Concentrating Solar Power Systems, $SCO_2$ Power Cycle Symposium, 2011.
[8] A. Moisseytsev, J.J. Sienicki, Analysis of Supercritical $CO_2$ Cycle Control Strategies and Dynamic Response for Generation IV Reactors, 2009. ANL-GenIV-124.
[9] B.T. Liu, K.H. Chien, C.C. Wang, J. Energy 29 (2004) 1207–1217.
[10] Y. Chen, P. Lundqvist, A. Johansson, P. Platell, J. Appl. Therm. Eng. 26 (2006) 2142–2147.
[11] Ernest G. Feher, in: The Intersociety Energy Conversion Engineering Conference, 1967.
[12] Yong Wang, G.R. Guenette, P. Hejzlar, M.J. Driscoll, Aerodynamic Design of Turbomachinery for 300MWe Supercritical Carbon Dioxide Brayton Power Conversion System, March 2005. Topical report, MIT-GFR-022.
[13] H.J. Yoon, Y. Ahn, J.I. Lee, Y. Addad, Nucl. Eng. Des. 245 (2012) 223–232.
[14] R.K. Shah, D.P. Sekulic, Fundamentals of Heat Exchanger, John Wiley & Sons, Inc., 2002.